Paper 5050-11, Proceedings of the SPIE Smart Structures Conference San Diego, CA., Mar 2-6. 2003

BAW and SAW sensors for In-situ analysis

Stewart Sherrit, Xiaoqi Q. Bao, Yoseph Bar-Cohen, and Zensheu Chang
Jet Propulsion Laboratory, Caltech, Pasadena, CA

ABSTRACT

In-situ planetary sample analysis is a major goal in current and future NASA exploration missions. In general in-situ analysis experiments are designed to investigate chemical, biological or geological markers or properties to determine the complex history of the body being studied or for use as a pre-screening measurement to increase the scientific value of samples selected for sample return. In order to expand the number of applicable sensor schemes and the available capability an investigation into piezoelectric bulk acoustic wave (BAW) and surface acoustic wave (SAW) resonators has been initiated with emphasis on applications to future NASA missions. In general, BAW and SAW sensors can be configured to directly measure mass, acoustic impedance, density and elastic property changes. Indirectly they can be designed to measure or monitor pressure, temperature, dew/melting point, curing, adsorption/desorption, and viscosity and be configured with the appropriate reaction layers as chemical sensors or as Immunosensors. The various models used to describe these sensors will be presented and the measurand sensitivity and importance of cross sensitivities will be discussed. Recent advances in passive wireless RF interrogated SAW technology has increased the scope of these sensor systems to remote sensing (10m) and to applications which may have been deemed previously inaccessible[1,2,3,4.] Examples include SAW stress sensors buried in large structures that once assembled are inaccessible for measurement that can be interrogated with wireless RF signals to determine the health of the structure. In addition, this technology has recently been coupled with other sensor technology allowing for an expansion of the possibilities for remote sensing. On the basis of the cost, range, versatility and ease of array fabrication, these sensors offer significant potential for future NASA missions.

Keywords: Piezoelectric, Ultrasonic, Bulk Acoustic Waves, Surface Acoustic Waves, RF interrogated sensors, microfluidics

1. INTRODUCTION

Due to the wide variety and number of NASA unmanned missions a need exists for instruments that can measure a wide range of properties under harsh conditions in remote locations with a maximal level of autonomy. These in-situ instruments and sensors need to be robust, stable and sensitive and are required for applications that range from micro analytical laboratories, to distributed sensor networks. In addition these instruments should be highly tolerable of temperature, pressure, radiation, and large acceleration/deceleration. The advantage of using resonators is that frequency is easy to measure accurately in an environment where ambient voltage levels may be large and random. In this paper we will discuss the application of BAW and SAW resonators and how they can be configured for multisensing and discuss the use of SAW devices in wireless passive designs to measure a wide variety of properties. Finally we will outline the possible applications for In-Situ analysis.

2. BAW SENSORS

Bulk Acoustic Wave (BAW) sensors based on the Quartz Crystal Microbalance (QCM)[5] have been used for many decades as thin film monitors in thermal evaportors, electrochemical deposition sensors, biosensors, chemical sensors, humidity sensors and immunosensors. The majority of these sensors are based on the thickness shear mode of AT cut quartz. A photograph of an AT cut quartz crystal and schematic examples of these sensors in different configurations are shown below in Figure 1. A variety of models are used to describe these resonators from simple lumped circuit models such as the Butterworth Van Dyke model to transmission line models like the Mason equivalent circuit for the thickness shear resonator shown in Figure 2.

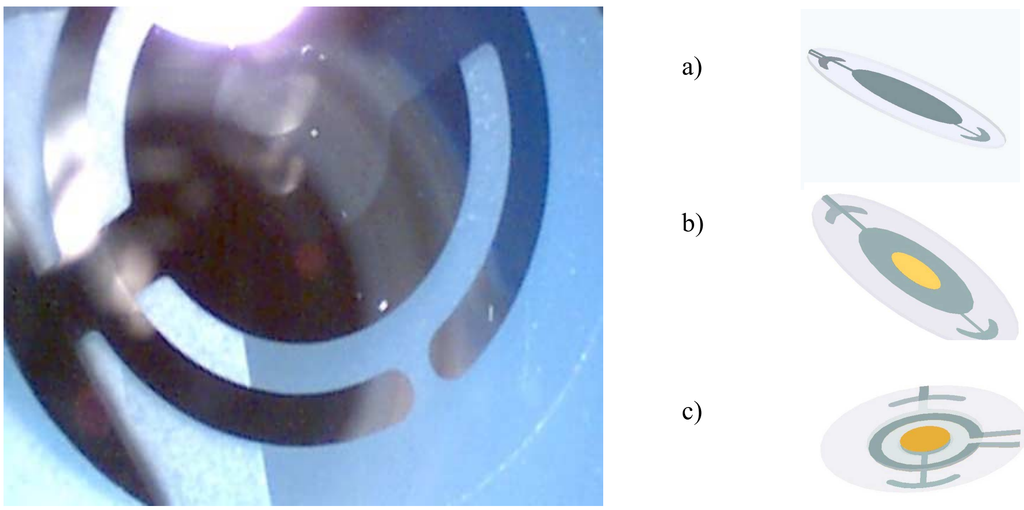

Figure 1. Examples of BAW resonators. a) Bare quartz crystal for monitoring deposition, b) Quartz crystal with reaction layer for monitoring chemical reaction, c) Quartz crystal with layer and heater for monitoring adsorption isotherms

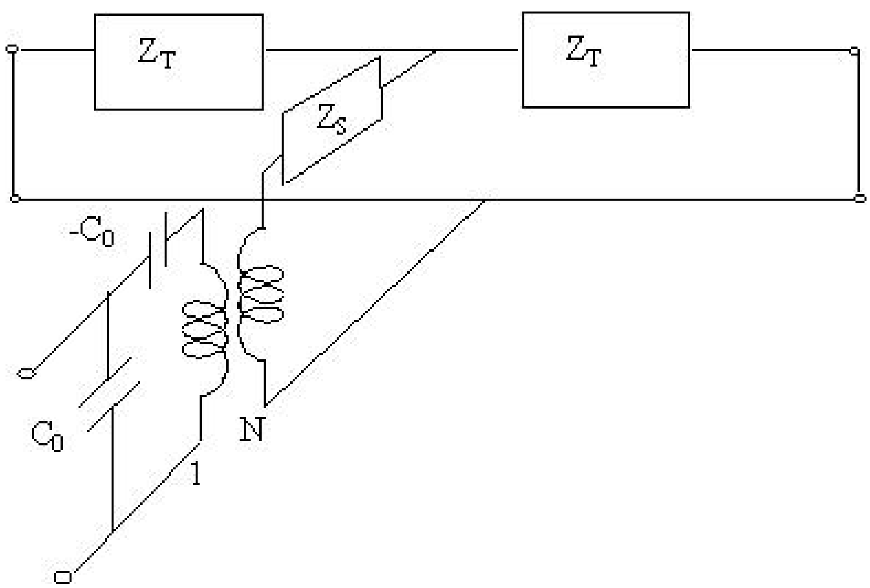

Figure 2: Mason's equivalent circuits with short circuits on the acoustic ports (unclamped-free resonator). Quantities in figure are defined in Table 1

The quantities of the model shown in Figure 2 and Figure 3 are defined in Table 1. The impedance of the acoustic layer if terminating is of the form $Z_L = i\rho v A \tan(\omega t/v)$ where A is the electrode area, *v* is the acoustic velocity of the shear wave in the layer, t is the layer thickness and ρ is the layer density. The parasitic element on the electrical port can be represented by a leaky capacitance and determined from the change in the baseline impedance before and after the deposition of the layer.

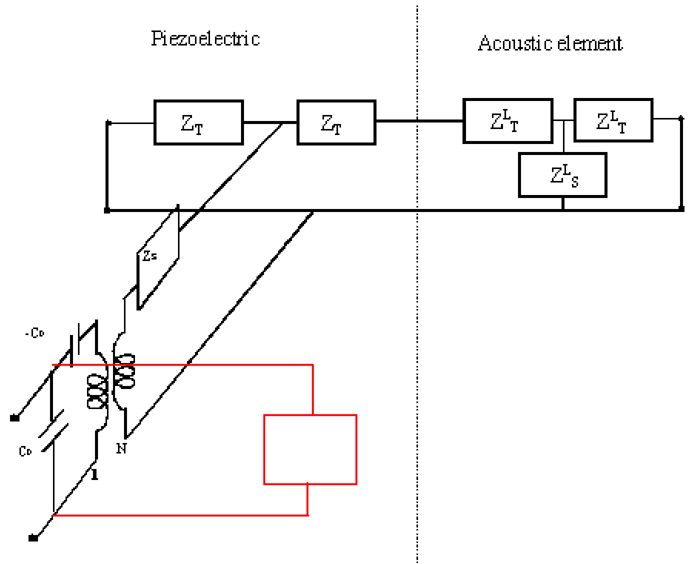

Figure 3. The transmission line model of a piezoelectric in the thickness shear mode with an acoustic layer. The layer is a network equivalent which can be simplified to a simple tan function if it is terminating. In addition to the acoustic load a parasitic electrical load may be present on the input electrical terminals due to the change in the electric boundary conditions (eg. polar liquid). Quantities in the figure are defined in Table 1.

Table 1. The complex material coefficients of Mason's equivalent circuit parameters and the equation and coefficients of the free resonator. The equations shown can be used to describe the thickness extensional and the thickness shear resonance mode.

Free Resonator

$$\mathbf{Z} = \frac{t}{i\omega A \boldsymbol{\varepsilon}^S}\left(1 - \frac{\mathbf{k}^2 \tan\left(\frac{t\omega}{2}\sqrt{\frac{\rho}{\mathbf{c}^D}}\right)}{\frac{t\omega}{2}\sqrt{\frac{\rho}{\mathbf{c}^D}}}\right)$$

$\boldsymbol{\varepsilon}^S$ clamped complex permittivity $\boldsymbol{\varepsilon}^S = \varepsilon_r^S + i\varepsilon_i^S$

$\mathbf{c}^D$ open circuit complex elastic stiffness $\mathbf{c}^D = c_r^D + ic_i^D$

$\boldsymbol{k}$ complex electromechanical coupling $\boldsymbol{k} = k_r + ik_i$

$$\boldsymbol{k}^2 = \boldsymbol{e}^2 / \mathbf{c}^D \boldsymbol{\varepsilon}^S = \boldsymbol{h}^2 \boldsymbol{\varepsilon}^S / \mathbf{c}^D$$

$$\boldsymbol{h} = \boldsymbol{k}\sqrt{\mathbf{c}^D / \boldsymbol{\varepsilon}^S}$$

Mason's Model

$$\mathbf{C}_0 = \frac{\boldsymbol{\varepsilon}^S A}{t} \qquad \mathbf{N} = \mathbf{C}_0 \boldsymbol{h}$$

$$\boldsymbol{Z}_0 = \rho A \mathbf{v}^D = A\sqrt{\rho\, \mathbf{c}^D} \qquad \boldsymbol{\Gamma} = \frac{\omega}{\mathbf{v}^D} = \omega\sqrt{\frac{\rho}{\boldsymbol{c}^D}}$$

$$Z_T = i\mathbf{Z}_0 \tan(\boldsymbol{\Gamma} t/2) \qquad Z_S = -i\mathbf{Z}_0 \csc(\boldsymbol{\Gamma} t)$$

Under the application of an AC signal on the electrodes of the piezoelectric quartz crystal the quartz vibrates in the thickness shear mode with the surfaces of the electrode moving in the direction of the electrode plane. Under no load conditions the crystal vibrates at its natural resonance frequency. If the surface of the crystal is attached mechanically to a thin film, fluid or structure the resonance shifts. In the limit of a thin film the sensor is mass loaded and a frequency shift that depends on the mass of the layer is found. The mass of the layer is determined from the Sauerbrey equation[6].

$$\Delta m = m_o \Delta f / f_o \tag{1}$$

where m_o is the mass of the electroded region of the resonator, f_o is the initial natural frequency of the resonator and Δf is the frequency shift after deposition. Typical sensitivity values are in the range of 10^{-9} grams assuming frequency resolution in the 0.2 Hz range

In previous work[7] we extended the Sauerbrey equation to a complex form where

$$\mathbf{m}^*(f_{S2}) = m_0 \frac{\left(f_{s1} + \Delta f_{s1} i\right) - \left(f_{s2} + \Delta f_{s2} i\right)}{\left(f_{s1} + \Delta f_{s1} i\right)} \tag{2}$$

m_o is the mass of the electroded resonator, f_{s1} and f_{s2} are the series resonance frequencies prior to the attachment of the acoustic layer and after the layer is attached and the Δf terms are the bandwidths about resonance(HWHM) of each resonance. $\mathbf{m}^*$ is the effective complex mass which depends on the type of acoustic layer. For example in the case of a Newtonian fluid with $v = (i\eta\omega/\rho)^{1/2}$ the acoustic layer is found by considering the fluid as a terminating impedance of infinite length.

$$\mathbf{Z}_L = i\rho_l A_l \mathbf{v}_l \tan\left(\frac{\omega L}{\mathbf{v}_l}\right) = i\rho_l A_l \mathbf{v}_l (-i) = \rho_l A_l \mathbf{v} = A_l \left(i\eta\omega\rho_l\right)^{1/2} = im^*\omega \tag{3}$$

This relationship can be illustrated from previously published data[7] on polished Quartz AT cut crystals from Maxtek Inc. (P/N 149240-1 nominal 5MHz Ti/Pt electrodes) that were mounted in the crystal holder. The impedance spectrum of the unperturbed quartz crystal was then measured using an HP 4192a Impedance analyzer. The quartz and the holder were then immersed in distilled water and the impedance spectrum of the quartz crystal in contact with the water was measured. The results are shown in Figure 4. The complex mass determined from the complex frequencies of the two spectra were $\mathbf{m}^* = 6.44\times10^{-9} - 6.03\times10^{-9}i$ kg with $\omega = 3.138\times10^7$ rads/s, $A = 4.195\times10^{-5}$ m^2, $\rho = 1000$ kg/m^3. Using equation 3 the viscosity is $\eta = 1.38(1+0.066i)$ Ns/m^2 which compares reasonably well with the book value of $\eta = 1.12$ Ns/m^2 at 60 ^{o}F. The complex part of η determined above is a measure of the experimental error (no correction for parasitic electrical component), surface roughness and deviations from pure Newtonian fluid.

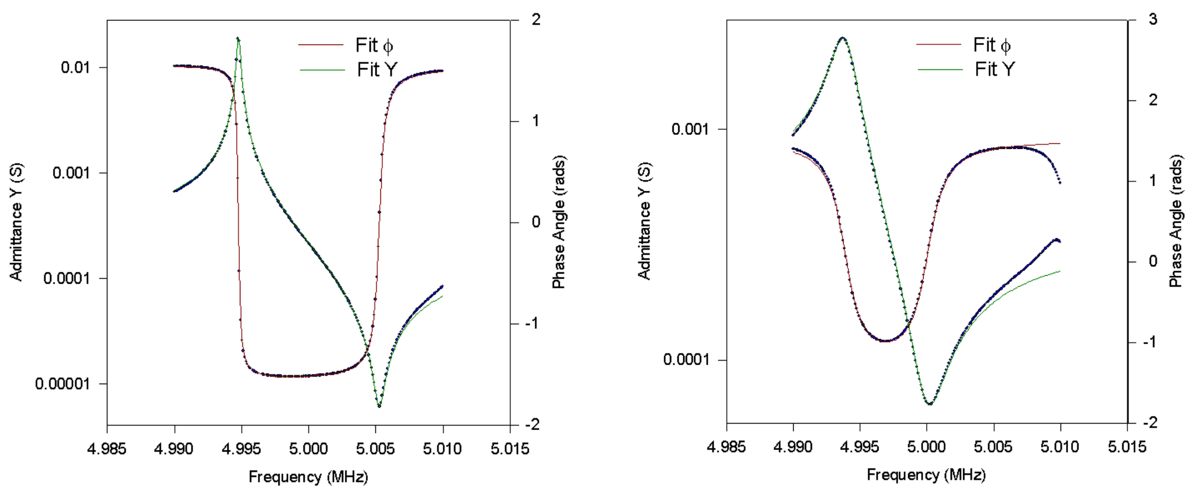

Figure 4. The admittance spectra of a 5 MHz Quartz crystal in air (left) and distilled water (right) and the resultant fit using complex material coefficients. There is almost a ten-fold decrease in the quality of the resonance when immersed in water.

2. SAW RESONATORS

A micrograph and schematic drawing of a typical SAW resonator is shown in Figure 5. Driving the interdigital transducers with opposing signal polarity generates the surface wave. The surface charge interacts with the piezoelectric substrate to produce the waves, which travel in the forward and reverse directions. These waves are then reflected by the reflectors (shown in Figure 5) into the IDT region. The amplitude of the wave increases until the rate of energy loss is equal to the input power of the signal.

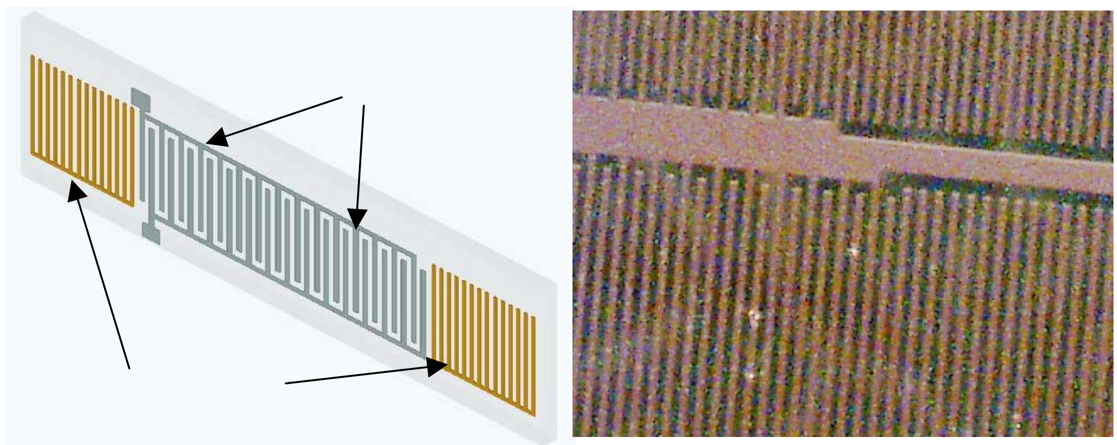

Figure 5. The figure shows a schematic diagram of a SAW resonator configuration. IDT's located between the reflectors excite surface wave which travel in the forward and reverse direction. Each line of the reflector partially reflects the wave back into the IDT's.

The micrograph of the IDT as can be seen in Figure 5 shows the IDT's of a dual SAW resonator and the reflectors, which are designed to resonate at 55.25 MHz (lower) and 62.25 MHz (upper) (Vanlong SR3-4B). Inter-digital transducers (IDT's) finger electrodes with opposing polarity on a piezoelectric substrate are driven at RF frequencies which causes the surface around the IDT's to distort creating a surface wave which travels at approximately 3000 m/s along the surface. Grid Reflectors at the ends of the device reflect the energy back to the IDT's in order to form high Q resonators. By adjusting the spacing between the electrodes the resonance frequency range of the sensors can be tuned. In addition to the properties above the SAW resonator can be design to have high Q (Q's =20,000-100,000), which allows for accurate determination of the frequency and frequency shifts. In addition a wide variety of materials are available with a range of pertinent properties as is shown in Table 2.

Table 2: SAW Properties of Common Materials (Yili Wu et al. "Principals of Surface Acoustic Waves and its application in Electronic Technology" Defense Industrial Press, PRC, 1983, (In Chinese)

Material	SAW velocity v (m/s)	Coupling K^2(%)	ε (pF/m)	α_T (ppm/°C)
Quartz ST-X	3158	0.16	55	≈0
$LiNbO_3$ (YZ)	3485	4.5	460	91
$LiNbO_3$ (128°)	3921	5.7	-	57
ZnO	2715	1	-	40
$Bi_{12}GeO_{20}$ (100) (011)	1681	1.5	400	130

The resonance equation for these devices is of the form

$$Y(\omega)=2\frac{\omega_0 c_s K^2}{2\pi}\left(\tan\left(\frac{\pi\omega}{2\omega_0}\right)\sin\left(N\frac{\pi\omega}{\omega_0}\right)\right)^2+i\omega N c_s+\frac{i\omega_0 c_s K^2}{2\pi}\tan\left(\frac{\pi\omega}{2\omega_0}\right)\left(4N+\tan\left(\frac{\pi\omega}{2\omega_0}\right)\sin\left(N\frac{2\pi\omega}{\omega_0}\right)\right) \qquad (4)$$

Where K = coupling factor, ω_0 = resonance frequency, c_S = capacitance of IDT pair and N = Number of electrode pairs. In terms of purely electrical components these devices are modeled using the Butterworth Van-Dyke circuit, which is a capacitance in parallel with a capacitance, inductance and resistance. These devices can be used for measuring small changes in the mass and elastic properties of a film as shown in Figure 6 by monitoring the change in the resonance frequency. The change in resonance is described by [8,9]

$$\frac{\Delta f}{f}=\kappa\Delta\left(-\frac{v}{4}\left(\frac{|v_y|^2}{P_r}+\frac{|v_z|^2}{P_r}\right)h\rho'+\left(h\mu\frac{\lambda+\mu}{\lambda+2\mu}\right)\left(\frac{1}{v}\frac{|v_z|^2}{P_r}\right)\right) \qquad (5)$$

where ρ' is the mass area density, κ is the percent area coverage, v is the Rayleigh mode velocity, $v_{y,z}$ are the surface velocity components, P_r is the acoustic power and λ,μ are Lames constants of film. The first term is the frequency shift due to mass effects while the second term is due to elastic effects.

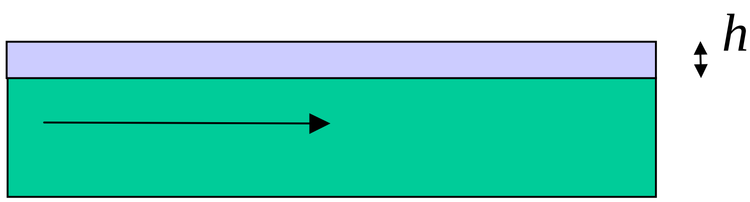

Figure 6. The figure shows a schematic diagram of a mass/elastic loaded SAW resonator with a film of thickness h.

3. MULTISENSING

Both BAW and SAW resonators can be configure in arrays to sense a variety of measurands or monitor a variety of other environmental properties (Temperature, Pressure, Humidity, etc.) that may affect the accuracy and stability of the measurement. As and example arrays of SAW and BAW resonators are shown below in Figure 7.

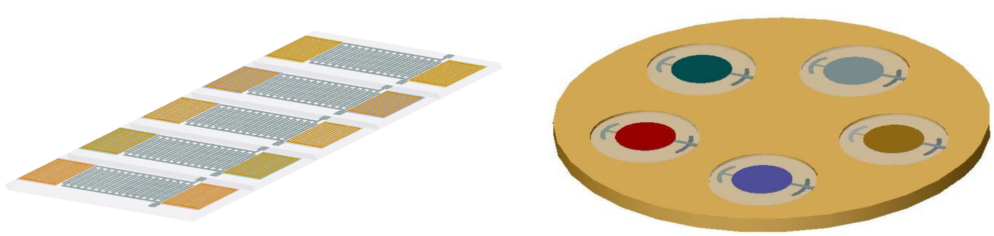

Figure 7. Schematic drawing of an array of SAW and BAW sensors used to sense a variety of measurands.

As with any sensor, cross-sensitivities can limit to the overall accuracy and sensitivity of the measurement[10,11,12]. It is therefore important to account for the environmental and other effects when designing multisensing units. As was pointed out in earlier work[13] these sensitivities can be written in terms of a linear equation with the coefficient equal to the normalized sensitivity. In general the total frequency shift of sensor i can be written in terms of the sum of the cross sensitivity $k_{i,j}$ and the magnitude of the physical property X_j.

$$\Delta f_i = k_{i,j} X_j \tag{6}$$

where $i \geq j$.

$$\begin{bmatrix} \Delta f_1 \\ \Delta f_2 \\ \Delta f_3 \\ \vdots \\ \Delta f_n \end{bmatrix} = \begin{vmatrix} k_{11} & k_{12} & k_{13} & k_{1j} & k_{1n} \\ k_{21} & k_{22} & k_{23} & k_{2j} & k_{2n} \\ k_{31} & k_{32} & k_{33} & k_{3j} & k_{3n} \\ k_{i1} & k_{i2} & k_{i3} & k_{ij} & \vdots \\ k_{n1} & k_{n2} & k_{n3} & \dots & k_{nn} \end{vmatrix} \begin{bmatrix} X_1 \\ X_2 \\ X_3 \\ \vdots \\ X_n \end{bmatrix} \tag{7}$$

The physical properties can therefore be determined from the inverse of the sensitivity matrix or

$$\begin{bmatrix} X_1 \\ X_2 \\ X_3 \\ \vdots \\ X_n \end{bmatrix} = \begin{vmatrix} k_{11} & k_{12} & k_{13} & k_{1j} & k_{1n} \\ k_{21} & k_{22} & k_{23} & k_{2j} & k_{2n} \\ k_{31} & k_{32} & k_{33} & k_{3j} & k_{3n} \\ k_{i1} & k_{i2} & k_{i3} & k_{ij} & \vdots \\ k_{n1} & k_{n2} & k_{n3} & \dots & k_{nn} \end{vmatrix}^{-1} \begin{bmatrix} \Delta f_1 \\ \Delta f_2 \\ \Delta f_3 \\ \vdots \\ \Delta f_n \end{bmatrix} \tag{8}$$

As an example consider the cross sensitivities for gas adsorption studies using SAW resonators as noted previously by Ballantine et al.[14] and Hietala et al.[13].

$$\frac{\Delta v}{v} = \frac{-\Delta\beta}{\beta} \approx \frac{\Delta f}{f} = k_m \frac{\Delta m}{m} + k_c \frac{\Delta c}{c} + k_T \frac{\Delta T}{T} + k_\gamma \frac{\Delta\gamma}{\gamma} + k_\sigma \frac{\Delta\sigma}{\sigma} \tag{9}$$

where v is the velocity, β is the propagation factor m is the mass, c is the elastic stiffness, T is the temperature, γ is the surface tension and σ is the film stress. Now if each of the sensors is designed with different materials or in some cases in a different resonant configuration the sensitivity to other variables can be corrected for and measured separately by writing equation 9 in matrix form and noting that each of the measurands can be determined by multiplying the frequencies of each of the resonators by the inverse of the matrix of normalized coefficients.

$$\begin{bmatrix} \Delta f_1 \\ \Delta f_2 \\ \Delta f_3 \\ \Delta f_4 \\ \Delta f_5 \end{bmatrix} = \begin{vmatrix} k_{m1} & k_{c1} & k_{T1} & k_{\gamma 1} & k_{\sigma 1} \\ k_{m2} & k_{c2} & k_{T2} & k_{\gamma 2} & k_{\sigma 2} \\ k_{m3} & k_{c3} & k_{T3} & k_{\gamma 3} & k_{\sigma 3} \\ k_{m4} & k_{c4} & k_{T4} & k_{\gamma 4} & k_{\sigma 4} \\ k_{m5} & k_{c5} & k_{T5} & k_{\gamma 5} & k_{\sigma 5} \end{vmatrix} \begin{bmatrix} \Delta m \\ \Delta c \\ \Delta T \\ \Delta\gamma \\ \Delta\sigma \end{bmatrix} \Rightarrow \begin{bmatrix} \Delta m \\ \Delta c \\ \Delta T \\ \Delta\gamma \\ \Delta\sigma \end{bmatrix} = \begin{vmatrix} k_{m1} & k_{c1} & k_{T1} & k_{\gamma 1} & k_{\sigma 1} \\ k_{m2} & k_{c2} & k_{T2} & k_{\gamma 2} & k_{\sigma 2} \\ k_{m3} & k_{c3} & k_{T3} & k_{\gamma 3} & k_{\sigma 3} \\ k_{m4} & k_{c4} & k_{T4} & k_{\gamma 4} & k_{\sigma 4} \\ k_{m5} & k_{c5} & k_{T5} & k_{\gamma 5} & k_{\sigma 5} \end{vmatrix}^{-1} \begin{bmatrix} \Delta f_1 \\ \Delta f_2 \\ \Delta f_3 \\ \Delta f_4 \\ \Delta f_5 \end{bmatrix} \tag{10}$$

In this method it assume in the range of the measurement that all responses are in a linear range and that the k values are known for each resonator. In practice this is very complicated and time consuming and in general the number of constants required to solve the multisensing system increases with the square of the number of measurands. However for measuring errors due to temperature or pressure changes this is reasonably straightforward method of correction and calibration. An alternative is to design sensors with insignificant cross sensitivities. Examples of this would be sensors that are isolated chemically and mechanically but kept in thermal contact with the sensor chamber (pure temperature measurement) or sensors, which are thermally and chemically isolated but kept in mechanically equilibrium using a diaphragm (pure pressure measurement). These designs are mathematically the equivalent of zeroing off diagonal elements for a sensor row.

5. REMOTE WIRELESS PASSIVE SENSING

In addition to the sensor configurations discussed above when the sensor location is at an unreasonable or varying distance or when the sensor is not easily accessible SAW sensors acting as delay lines can be configured to be passive and wireless allowing for a remote measurement of the measurand from the control center. Designs of SAW devices from the 10's MHz to the GHz range have been demonstrated. Since the waves essentially travel along the surface (attenuation is exponential into the substrate) the ultrasonic waves can be confined to an area on the surface which is isolated from any load points (example substrate can be bonded to a beam with little perturbation on the resonator. In this configuration surface acoustic wave devices offer a variety of unique advantages over other sensor materials.

The SAW devices discussed above can be configured in to produce a delay line which can be excited remotely from an RF source by connecting the input electrodes to a receive antennae. If reflectors are placed at appropriate distances along the substrate a signal will be reflected back to the IDT and excite the antennae which broadcasts the pulse back to the RF source. If two or more reflectors are placed along the substrate and the time (or phase) between reflected pulses is monitored one can determine to high accuracy the wave traveling time between reflectors. This result has been used by a variety of authors to create wireless passive SAW stress, strain and temperature sensors[1,2,3,4,15] by monitoring the spacing change as a function of a external perturbing variable (Temperature, Stress etc.) These sensors are rugged, lightweight (<10g) and have demonstrated temperature sensitivities of 0.3 ^{o}C and force sensitivities in the milligram to kg range depending on the transducer design. A generalized schematic of the system is shown in Figure 8. Currently these systems are available commercially[16] for remote card reading of digital data as used at secure facilities and toll bridges and operate up to a range of 10-15 m.

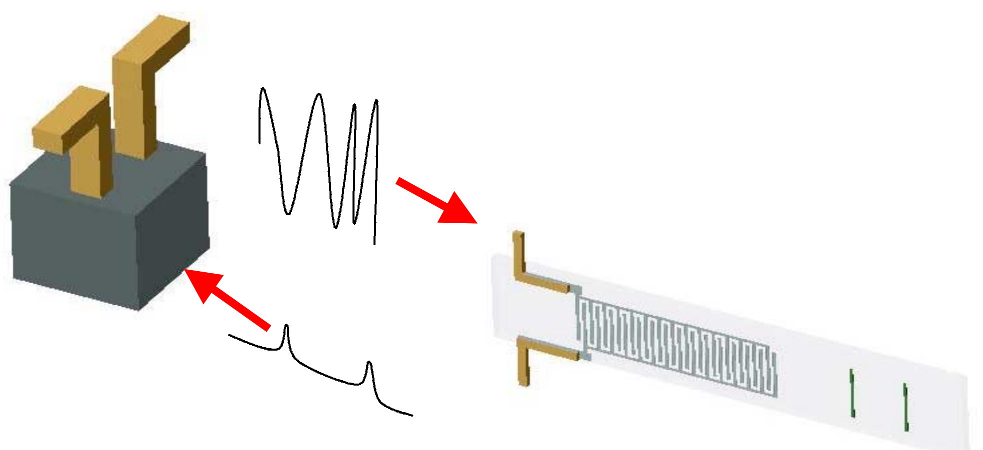

Figure 8. Schematic of a SAW delay line configured to measure change in phase of reflected pulses (time between successive reflections). If configured in a cantilever and a tip force is applied the change in phase is a measure of the strain in the crystal and can be converted to stress using beam theory.

6. SENSOR PLATFORMS

One of the important NASA objectives of the planetary exploration program is to conduct in-situ science that includes mineralogical and chemical analysis (e.g. water detection), and biological signature identification. In addition spacecraft integrity (structural stress/strain, acceleration) and environmental factors (Temperature, Pressure, Humidity) need to be monitored A critical element of this objective is the availability of effective and reliable sensors that are sensitive, robust, and capable of providing information about a variety of independent variables. These sensors should consume low power and allow for miniaturization. Bulk Acoustic Wave (BAW) and Surface Acoustic Wave (SAW) resonators can be configured in a variety of designs to meet these requirements. These sensors are found to have sensitivities in the nano-gram range and they can be used to test both gas and liquid samples. In recent years numerous configurations of such sensors have been reported and used to measure environmental properties such as temperature, pressure, stress, acceleration, field and charge. In addition through the choice of suitable interactive layers these sensors can be design to measure the presence of a countless number of different atoms/molecules. Examples include basic physics experiments such as monitoring the deposition of monolayers, biochemical applications such as monitoring DNA mutations and commercial application like monitoring the "quality of beer" (see Table 3.). In addition to chemical and biological sensors these materials have also been configured to measure physio-chemical properties such as dew/melting point, curing, adsorption/desorption and viscosity. One of the major advantages of these sensors is the possibility of designing a variety of sensor heads that monitor a wide range of properties while using the same drive/measurement electronics. A study is underway at JPL's NDEAA lab to enhance the capability and accuracy of these sensors and to investigate the feasibility of these sensors to form "lab on a chip" designs. In addition we are currently investigating the use of the wireless passive SAW devices 100 m interrogation range for the measurement of mechanical variables such as stress and strain in large Gossamer structures.

Table 3. Condensed Literature Survey of sensor configurations using BAW and SAW devices

Physical Property	**BAW (Reference)**	**SAW (Reference)**
Mass	5,6,7	8,9
Temperature	17	1*
Humidity	18	19*
Viscosity	20	21,
Elastic Constant	7	9
Stress/Strain/Pressure	22	2,3,4,15
Acceleration	23	24,25
Chemical/Biological Property		
Adsorption	26	27
Reaction Rates		
Curing	7,28	
Phase Change		
Reactivity	29	
Immunosensors / biosensors	30, 31, 32	33,34
	* Configured in Wireless Design	

7. CONCLUSIONS

The physical acoustics of the BAW and SAW devices required for the fabrication and analysis of these devises as sensors was discussed and techniques to correct for cross sensitivities when using multisensing were presented. An alternative method based on the complex version of the Sauerbrey equation was presented which was found to be in agreement with the complex mass determined at the resonance frequency of the perturbed resonator. An initial survey of the sensor modes that are involved with the use of BAW and SAW was presented and a preliminary discussion of the configuration of passive wireless SAW devices suggest that these devices meet many of the requirements of future NASA missions

ACKNOWLEDGEMENTS

Research reported in this manuscript was conducted at the Jet Propulsion Laboratory (JPL), California Institute of Technology, under a contract with National Aeronautics Space Agency (NASA). The authors would like to thank Patricia Beauchamp of the In Situ Exploration and Sample Return Center of Excellence at JPL for her support.

REFERENCES

[1] X. Q. Bao, W. Burkhard, V. V. Varadan and V. K. Varadan, "SAW Temperature Sensor and Remote Reading System" Proceeding of the IEEE International Symposium on Ultrasonics, pp. 583-585, 1987

[2] V. V. Varadan, V. K. Varadan, X. Q. Bao, S. Ramanathan, D. Piscotty, "Wireless Passive IDT Strain Microsensor", Smart Materials and Structures, **6**, pp. 745-751, 1997

[3] A. Pohl, R. Steindl, L. Reindl, "The "Intelligent Tire" Utilizing Passive SAW Sensors- Measurement of Tire Friction", IEEE Trans. on Instrumentation and Measurement, **48**, pp. 1041-1046, 1999

[4] L. Reindl et al., (1998) " Theory and Application of Passive SAW Radio Transponders and Sensors" IEEE Trans. of UFFC, **45**, pp.1281-1292.

[5] R.W. Cernosek, S.J. Martin, A.R. Hillman, H.L Bandy, "Comparison of the Lumped-Element and Transmission-Line models for the Thickness-Shear-Mode Quartz Resonator Sensors, IEEE Trans. on Ultrasonics, Ferroelectrics and Frequency Control, **45**, 5, pp. 1399-1407, Sept.,1998

[6] G. Sauerbrey, "Verwendung von Schwingquarzen sur Wägung Dünner Schichten und zur Mikrowägung –*Translation* - Use of vibrating quartz for weighing of thin layers and for micro weighing", Z. Physik, 155, pp. 206-222, 1959

[7] S. Sherrit, V. Olazábal, J.M. Sansiñena, X. Bao, Z. Chang, Y. Bar-Cohen, "The use of Piezoelectric Resonators for the Characterization of Mechanical Properties of Polymers", Proceedings of the SPIE Smart Structures Conference, Vol. 4695, Paper No. 35, San Diego, CA., March 2002, SPIE

[8] B.A. Auld, Acoustic Fields and Waves in Solids Vol. II, 1973

[9] Susan L.Hietala, Vincent M. Hietala and Jeffrey Brinker, "Dual SAW Sensor Technique for Determining Mass and Modulus Change", IEEE Trans UFFC **48**, pp. 262-267)

[10] Kerstin Schroeder, Wolfgang Ecke, Rudolf Mueller, Reinhardt Willsch and Andrey Andreev, "A fibre Bragg grating refractometer", Meas. Sci. Technol. **12,** pp. 757–764, 2001

[11] Fleischer M, Simon E, Rumpel E, Ulmer H, Harbeck M, Wandel M, Fietzek C, Weimar U, Meixner H, "Detection of volatile compounds correlated to human diseases through breath analysis with chemical sensors", Sensors And Actuators B-Chemical, 83 (1-3), pp. 245-249 , 2002

[12] Vlasov Y, Legin A, Rudnitskaya A, "Cross-sensitivity evaluation of chemical sensors for electronic tongue: determination of heavy metal ions", Sensors And Actuators B-Chemical, 44 (1-3), pp. 532-537, 1997

[13] Susan L.Hietala, Vincent M. Hietala and Jeffrey Brinker, "Dual SAW Sensor Technique for Determining Mass and Modulus Change", IEEE Trans UFFC **48**, pp. 262-267)

[14] D.S. Ballantine, R.M. White, S.J. Martin, A.J. Ricco, E.T. Zellers, G.C. Frye, and H. Wohltjen, Acoustic Wave Sensors: Theory Design and Physico-Chemical Applications, Academic Press, San Diego, 1997

[15] W. Cheng, Y. Dong, and G. Feng, "A Multi-Resolution Wireless Force Sensing System Based upon a Passive SAW Device" IEEE Transactions on Ultrasonics, Ferroelectrics and Frequency Control. **48**, pp. 1438-1441, 2001

[16] XCI Inc., San Jose, CA.

[17] M. Nakazawa, T. Takemae, A. Miyahara, K. Matsuyama," **A** Study of Quartz Temperature Sensors Characterized by Ultralinear Frequency-Temperature Responses", IEEE Transactions On Sonics And Ultrasonics. Vol. **Su-32**., 6**,** pp. 828-834, 1985

[18] M. Kuroiwa, Y. Shimamoto, Y. Yasuda, S. Wakamoto and M. Nakazawa," Hysteresis Characteristics Vs Relative Humidity For At-Cut Quartz Humidity Sensors", Proceedings of the IEEE Frequency Control Symposium, pp. 492-496, 2001

[19] Hollinger, Richard D.; Tellakula, Anikumar R.; Li, C.-T.; Varadan, Vasundara V.; Varadan, Vijay K. "Wireless surface-acoustic-wave-based humidity sensor", Proc. SPIE Vol. 3876, p. 54-62, 8/1999

[20] K. Kwon, J.W. Evans ,"Viscosity changes of Li battery electrolytes and their long-term effect on the frequency of EQCM electrodes", Electrochemical And Solid State Letters **5** (3): A59-A61, 2002

[21] T. NOMURA, T. YASUDA," Measurement Of Acoustic Properties Of Liquids Using SH-Type Surface Acoustic Waves", Proceedings of the IEEE Ultrasonics Symposium, pp. 307-310, 1990

[22] R.J. Besson, J.J. Boy, B. Clotin, **Y.** Jinzaki, B.K. Sinha, and M**.** Valtlois, "A Dual-Mode Thickness-Shear Quartz Pressure Sensor", Proceedings of the IEEE Ultrasonics Symposium, pp485-493, 1991

[23] C. L. Anderson," Acceleration Charge Sensitivity In At-Quartz Resonators", Proceedings of the IEEE Frequency Control Symposium, pp. 519-529, 1995

[24] R. Clive Woods, Hoshi Kalami, and Brian Johnson, "Evaluation of a Novel Surface Acoustic Wave Gyroscope**",** IEEE Transactions On Ultrasonics, Ferroelectrics, And Frequency Control, **49**, 1, pp. 136-141, 2002

[25] Varadan, Vijay K.; Varadan, Vasundara V.; Bao, Xiao-Qi , "IDT, SAW, and MEMS sensors for measuring deflection, acceleration, and ice detection of aircraft", , Proc. SPIE Vol. 3046, p. 209-219, Smart Structures and Materials 1997: Smart Electronics and MEMS, Vijay K. Varadan; Paul J. McWhorter; Eds. , 6/1997

[26] Y Kim, D. E. Pierce, "Sensing Of Organic Vapor Adsorption On Gold Using A Temperature Insensitive Microbalance'', Proceedings of the IEEE Frequency Control Symposium, pp. 1001-1003, 1999

[27] I.V. Anisimkin, V. I. Anisimkin, F.S.Hickernell, "Novel Multi-Channel Saw Tool For The Analysis OfGas-Phase Adsorption" Proceedings of the IEEE Ultrasonics Symposium, pp. 331-335, 2001

[28] J.S. Schoenwald, M. Kendig and Dennis Tench, ''Resonating Disk Sensor For Conductive Ink Cure Monitoring'', Proceedings of the IEEE Ultrasonics Symposium, pp. 631-633, 1989

[29] Laik B, Poizot P, Tarascon JM,"The electrochemical quartz crystal microbalance as a means for studying the reactivity of Cu2O toward lithium", Journal Of The Electrochemical Society **149** (3): A251-A255 MAR 2002

[30]Chou SF, Hsu WL, Hwang JM, Chen CY, "Determination of alpha-fetoprotein in human serum by a quartz crystal microbalance-based immunosensor", Clinical Chemistry, 48 (6): 913-918 Part 1 JUN 2002

[31] Chen YK, Xiao D, Yang XH, Shao GQ, "Development of a piezoelectric immunosensor for hepatitis B surface antigen", Chen ZZ, Wang KM, , Chemical Journal Of Chinese Universities-Chinese, 23 (6): 1044-1046 JUN 2002

[32] Muramatsu H, Kim JM, Chang SM, "Quartz-crystal sensors for biosensing and chemical analysis", Analytical And Bioanalytical Chemistry, **372** (2): 314-321 JAN 2002

[33] N. Barie, M. Rapp, H. Sigrist, The Use Of Dextran As An Intermediate Layer: A New Approach Towards Saw Based Biosensors", Proceedings of the IEEE Frequency Control Symposium, pp. 997-1000, 1999

[34] J. Kondoh , *Y .* Matsui And S. Shiokawa, ''SH-Saw Biosensor Based On Ph Change'', Proceedings of the IEEE Ultrasonics Symposium, pp. 337-340, 1997